

Adjustment of conformation change and charge trapping in ion-doped polymers to achieve ternary memory performance†

Cite this: *J. Mater. Chem. C*, 2013, **1**, 7883

Dongwei He,^a Hao Zhuang,^a Haifeng Liu,^a Hongzhang Liu,^a Hua Li^{*a} and Jianmei Lu^{*ab}

Ion-doped poly(4-vinylpyridine) derivatives (**P4VPCz**), where in the pendant chains the electron-withdrawing pyridine moiety and acceptor carbazole moiety are linked by a flexible alkyl spacer were designed and synthesized. Sandwiched ITO/**P4VPCz**/Al devices, made through simple spin-coating processes have shown that they could be tuned from a binary to ternary memory performance, by increasing the carbazole content. **P4VPCz2** with a 20% mole ratio of the carbazole moiety shows a binary performance according to the charge trapping of the pyridine acceptor in the polymer, while **P4VPCz5** which contains a 50% mole ratio of carbazole in the pendant chains, exhibits a ternary data storage ability, probably induced by double mechanisms (*i.e.* a conformational change and charge trapping). Interestingly, as the carbazole mole ratio reached 80%, the polymer **P4VPCz8** has a high conductivity state, with no switching behavior, because of the large amount of doped ions improving the charge transfer mobility. Thus, we hope can offer a guideline to achieve a high-performance multilevel memory material, *via* combining different mechanisms as well as doping ions.

Received 7th September 2013

Accepted 3rd October 2013

DOI: 10.1039/c3tc31759e

www.rsc.org/MaterialsC

Introduction

Polymer-based electrically bistable devices are rather attractive nowadays for their potential applications in organic memory, due to their advantages of low operating voltage, rich structural flexibility, solution processability and three-dimension stacking capability.¹ Confronted with the ever-increasing requirements of super high density data storage in the coming message explosion era,² recently, several ternary memory devices based on small-molecule materials emerged through incorporating two different charge traps in one molecular backbone, leading to an exponential increase in data storage capacity relative to the binary memory systems.³ However, such devices based on polymeric materials were scarcely reported, probably because of the lack of appropriate design principles.⁴ The strategy of combining more than one mechanism in one device (*e.g.* charge transfer and metal filament formation,^{4a,b} conformational change and charge transfer^{4c}) has been effectively demonstrated to achieve ternary memory performances. To date, the operating

process of the ternary device is still unclear and thus more investigation should be focused on this perspective to help researchers gain more insight.

Herein, we designed and synthesized ion-doped poly(4-vinylpyridine) derivatives (**P4VPCz**) containing pyridine and carbazole moieties in the lateral chain. In poly(vinylpyridine) (**P4VP**), the electron-withdrawing pyridine moieties can not only act as charge trapping sites,⁵ but also provide active points to graft bromoethyl-carbazole moieties with ionic bonds. So, it is easy for charge transfer and charge trapping to occur in **P4VPCz**.⁶ Besides, a flexible alkyl spacer was intentionally introduced between the pendent carbazole moiety and the pyridine ring to hopefully induce the conformational change of the planar carbazole moieties when applying an external electric field.⁷ The result shows that when a 50% mole ratio of bromoethyl-carbazole was connected to the pyridine moieties, the sandwiched ITO/**P4VPCz5**/Al device exhibited ternary data storage characteristics, which was shown to be under a double mechanism, synergistic effect (*i.e.*, conformational change and charge trapping). Besides, the ions produced by bromoethyl-carbazole reacting with pyridine are helpful to achieve a balanced charge injection and transport throughout the active layer, thereby enhancing the carrier mobility and improving the device stability.^{8,9} However, once the doped-ions reached a certain amount, the memory device only showed a high conductivity state with no switching phenomenon, owing to the improved charge transfer

^aCollege of Chemistry, Chemical Engineering and Materials Science, Collaborative Innovation Center of Suzhou Nano Science and Technology, Soochow University, Suzhou 215123, P. R. China. E-mail: lujm@suda.edu.cn; Fax: +86 512 65880367; Tel: +86 512 65880368

^bState Key Laboratory of Treatments and Recycling for Organic Effluents by Adsorption in Petroleum and Chemical Industry, Suzhou 215123, P. R. China

† Electronic supplementary information (ESI) available: The compositions of the copolymers, SEM image, AFM, stability test of **P4VPCz2** and *I-V* characteristics, theoretical conduction models. See DOI: 10.1039/c3tc31759e

mobility. Therefore, the contribution of conformational change and charge transfer between the pyridine acceptor and carbazole donor in the **P4VPCz** tuning the device from binary to ternary and the doped ions enhancing the devices' stability may a guide the design and synthesis of stable multilevel memory materials in the future.

Results and discussion

The synthetic route of **P4VPCz** is shown in Scheme 1. The chemical structures were confirmed by ^1H NMR spectroscopy (see Fig. 1). The aromatic peaks of the carbazole rings could be noted for **P4VPCz**, compared to the ^1H NMR spectra of **P4VP**. The compositions of the copolymers (*i.e.*, the content of each moiety) were determined from the UV-vis absorption according to the standard curve of carbazole in DMF (Fig. S1, see the ESI †). The thermal properties of **P4VPCz** were investigated by TGA measurements. All the polymers exhibited good thermal stability with thermal decomposition temperatures (5% weight loss) over 270 $^\circ\text{C}$, implying that the copolymers are able to endure heat deterioration in the memory devices.

The sandwich structure of the memory device is illustrated in Fig. 2a. High-quality polymer thin films could be prepared through spin-coating. Fig. 2b shows the AFM image of **P4VPCz2** on an ITO substrate, which is quite smooth with a root-mean square (RMS) roughness of *ca.* 2.0 nm (Fig. 2c). The observed smooth morphology of the thin films is beneficial for the hole injection from the ITO into the HOMO of the polymers. 10

The effects of various compositions of poly(4-vinylpyridine) derivatives (**P4VPCz**) on the device memory performance were systematically investigated. The typical I - V characteristics of the ITO/**P4VPCz2**/Al device are shown in Fig. 3a. During the first sweep, from 0 to -6.0 V, the device was initially in the low-conductivity state (OFF state) with a slowly increasing current; then an abrupt leap in the current was observed at a threshold voltage ($V_{\text{th,s}}$) around -3.3 V, indicating the transition from the low-conductivity state (OFF state) to the high-conductivity state (ON state). This OFF-ON transition response to an external voltage can be utilized to store data in those electrical memory devices. After a subsequent sweep from 0 to -6.0 V (or 6.0 V), the memory device remained in the ON state and could not return to the original OFF state, whether by removing the electric field or applying a reverse voltage scan (0 to 6 V). These results demonstrate that the memory device fabricated with **P4VPCz2** exhibited a binary write-once-read-many-times

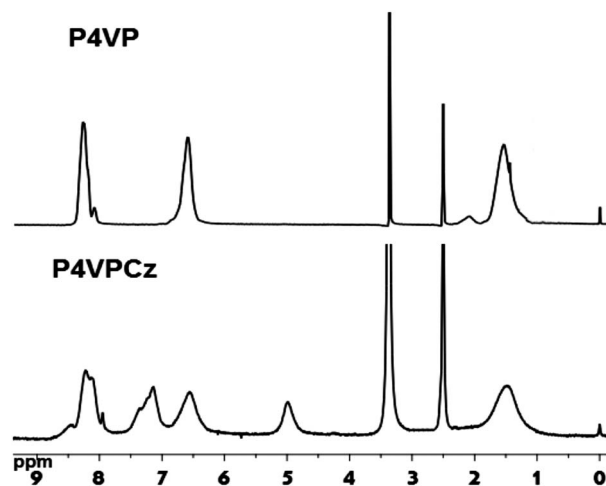
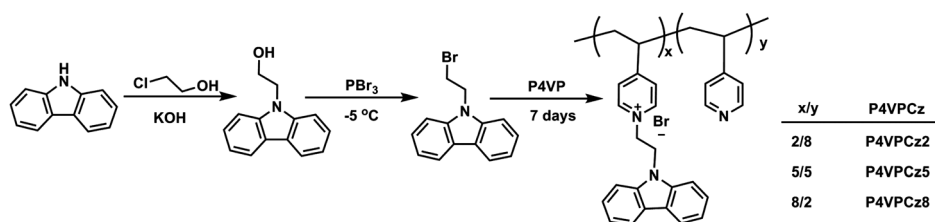


Fig. 1 ^1H NMR spectra of **P4VP** and **P4VPCz** in DMSO.

(WORM) memory behavior with an ON/OFF current ratio of approximately 10^7 . Compared with **P4VPCz2**, the electric behavior of the **P4VPCz5**-based device is rather different, exhibiting three distinct conductance states (Fig. 3b). Similarly, the bias is applied in a sequence of 0 to -6.0 V, two abrupt increases in the current could be observed around -2.5 V and -3.5 V, respectively, indicating that the device underwent two electrical transitions, the OFF state to an intermediate state (ON1 state) and then to a high-conductivity state (ON2 state). After the two transitions were achieved, the device was found to maintain the ON2 state, even after the power was turned off or by applying a reverse bias. These results suggest that the **P4VPCz5**-based device could be used as a nonvolatile ternary WORM device. It should be worthy of note that the $V_{\text{th,s}}$ is very uniform and stable after testing a large number of memory cells (Fig. S8, ESI †). In addition, segmented sweeps were also carried out from 0 to -3.0 V and 0 to -6.0 V, to study whether the programmed ON1 and ON2 states were erasable. The obtained ON1 and ON2 states were unable to be erased by reverse voltages. With a further increase in the content of carbazole moieties in the pendant chains, the **P4VPCz8** thin film showed only a single high-conductivity state, with no switching phenomenon, which indicates that when the carbazole moiety mole ratio reaches 80%, the device has no data storage ability. In summary, the electrical properties of **P4VPCz** devices were found to vary from binary to ternary and further to a conductor behavior with the content of carbazole and doped ions increasing.



Scheme 1 Synthetic route and molecular structure of **P4VPCz**.

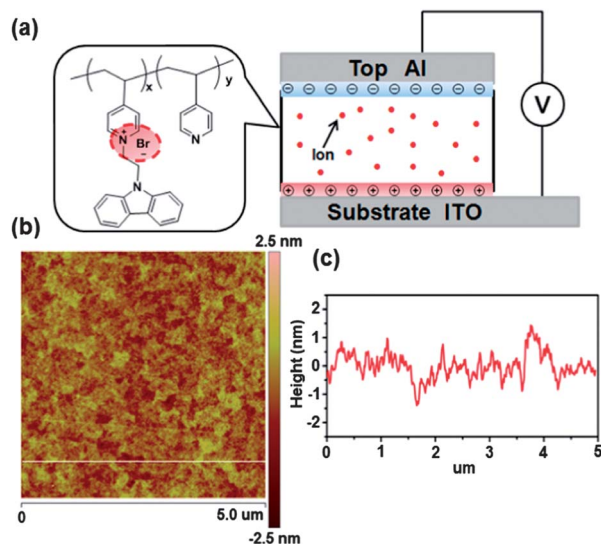


Fig. 2 (a) A schematic diagram of the ITO/P4VPCz2/Al device; (b) the tapping-mode ($5 \mu\text{m} \times 5 \mu\text{m}$) AFM topography image of P4VPCz2 on an ITO substrate; (c) roughness of the (b) thin film.

The long-term stability and endurance performance were also evaluated from the retention time and stimulus effect test. Fig. 4 shows that the P4VPCz5 device could endure over 10^8 continuous read pulses of -1.0 V and no significant degradation in the current for any state was observed for 100 min. The retention time and pulse endurance test of P4VPCz2 at -1.0 V also showed good stability (Fig. S4, ESI[†]). It is noteworthy that the writing voltages are all smaller than -4.0 V and the reading voltage is as low as -1.0 V, which imply a low power consumption of the P4VPCz device during practical data storage processes.

The P4VPCz containing different carbazole content, showing different memory performance was precisely discussed. The P4VPCz2 which only contains a 20% mole ratio of carbazole moieties shows a WORM memory effect, which we deduced was arising from the charge trapping process. As is well known, pyridine is an electron acceptor group and could act as a charge trapping site when the carriers were injected, under an electric field. After the charge traps were filled to full, the device exhibited an OFF to ON transition. In order to exclude that the OFF to ON transition of the P4VPCz2 based device was not contributed to by the charge transfer between the pyridine acceptors and the carbazole donors, the UV-visible spectra and the cyclic voltammetry (CV) curves of the P4VPCz thin films were examined. As can be seen from Fig. 5a, the P4VPCz film shows three strong absorption bands centered at 298, 331 and 344 nm, which is consistent with the spectral features of carbazole. The absorption of the copolymers with different compositions exhibited no significant change, indicating the weak intramolecular charge transfer between the carbazole donor and the pyridine acceptor within the film.¹¹ Furthermore, Fig. 5b shows that in a solution of dichloromethane with tetrabutylammonium perchlorate (TBAP) (0.1 M) as the electrolyte at a scan rate of 100 mV s^{-1} , all the polymers exhibit an irreversible oxidation behavior with the first oxidation peaks in the range 1.38–

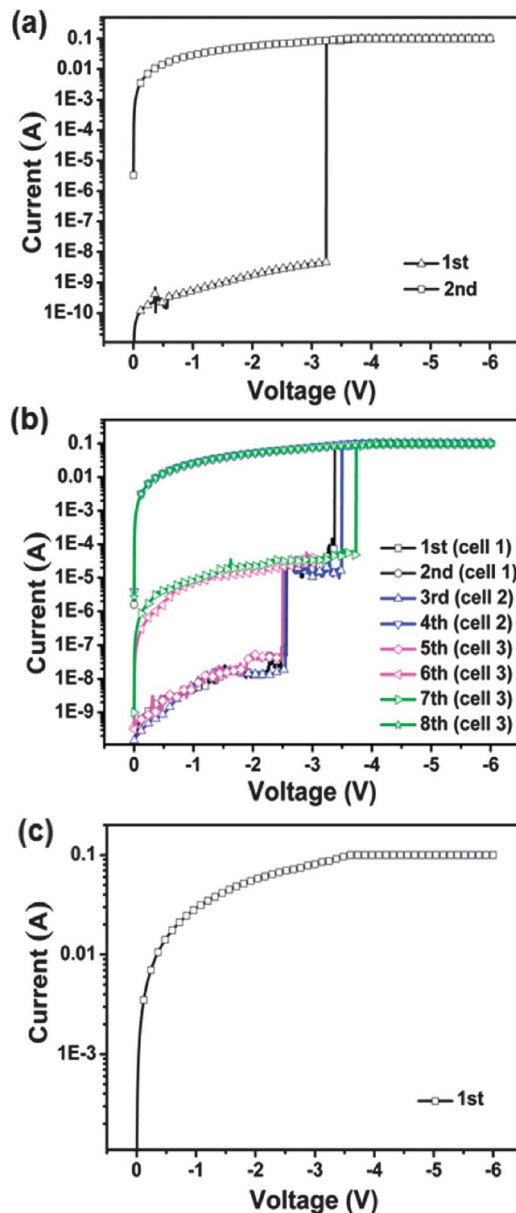


Fig. 3 I - V characteristics of (a) ITO/P4VPCz2/Al, (b) ITO/P4VPCz5/Al and (c) ITO/P4VPCz8/Al devices.

1.28 eV. The HOMO and LUMO energy levels of the polymer were estimated from the CV results with reference to ferrocene (4.8 eV) by the following equations:

$$E_{\text{HOMO}} = -[E_{\text{ox}}^{\text{(onset)}} + 4.8 - E_{\text{Ferrocene}}]$$

$$E_{\text{LUMO}} = E_{\text{HOMO}} + E_{\text{g}}$$

$$E_{\text{g}} = hc/\lambda_{\text{Edge}}$$

The HOMO and LUMO energy levels are summarized in Table 1. The slight fluctuation also clarified that the charge transfer between the carbazole donor and pyridine acceptor is relatively weak, suggesting that the observed memory

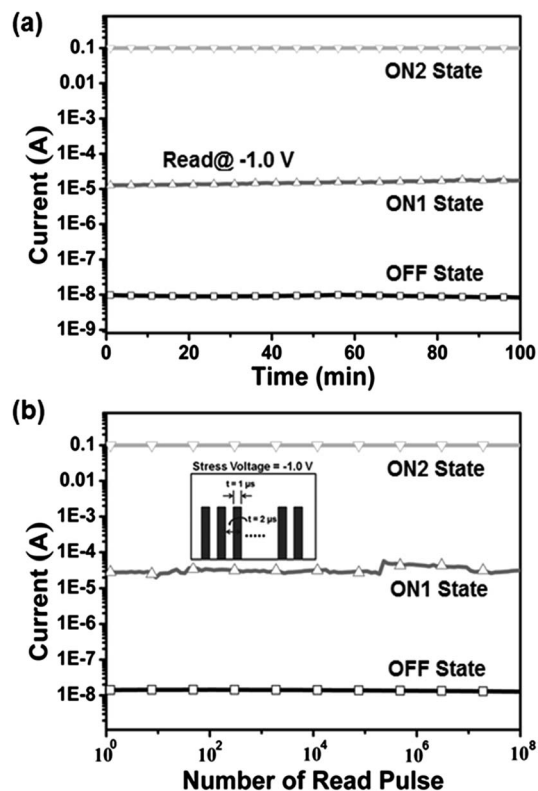


Fig. 4 Stability test of the ITO/P4VPCz5/Al device. (a) Retention time of the OFF, ON1 and ON2 states under a continuous readout voltage (-1.0 V); (b) stimulus effect of a read pulse of -1.0 V on the three distinct states. The inset shows the pulse shapes adopted in the measurement.

performance (for P4VPCz2) originated from the pyridine trap, instead of the charge transfer effect.¹²

Kang *et al.* have demonstrated that the pendant polymers containing an electroactive chromophore in the side-chains, such as the carbazole (Cz), naphthalene (Na) and anthracene (An) moieties or π -conjugated moieties, exhibited electrical bistability controlled by the electric-field-induced conformational change, and the different memory characteristics are decided by the flexible spacer between the polymer backbone and the functional chromophore.¹³ Herein, the designed P4VPCz contains a flexible spacer and as long as the carbazole moieties reach a certain number, conformational change will certainly take place under an electric field. As for P4VPCz5 with a relatively high carbazole ratio, under a low voltage bias (0 to -2.5 V), holes started to inject from the ITO to the carbazole segment near the interface, forming active species. The neighboring neutral carbazole groups tended to distort and form a partial or full face-to-face conformation attracted by the active carbazole species. Then, the charge was delocalized to the neighboring carbazole groups through a more ordered conformation. It is better for charge carrier transportation to form free channels under an electrical field, but the carriers do not have sufficient energy to overcome the barrier of the pyridine trap and are blocked by the electron-accepting pyridine moieties in the film, thus only exhibiting the intermediate state. With the voltage further increasing, traps of the pyridine moieties were gradually

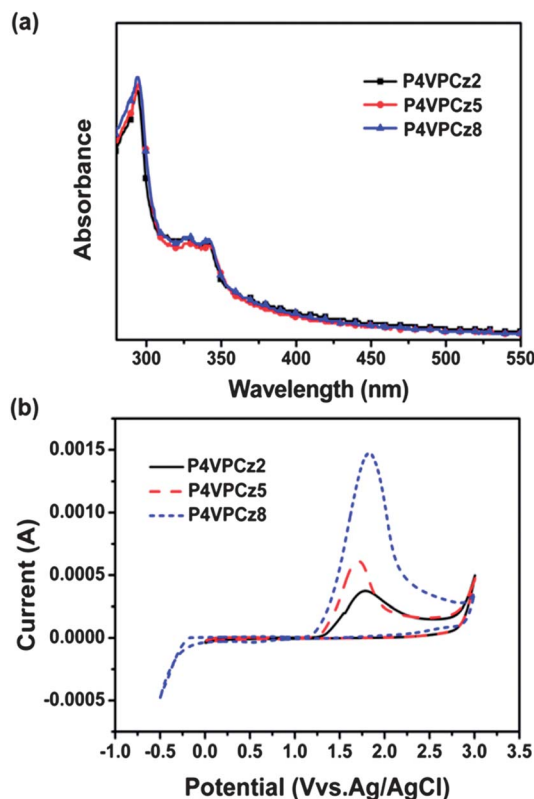


Fig. 5 (a) UV-visible absorption spectra of the P4VPCz films on a quartz plate; (b) cyclic voltammogram of P4VPCz thin films spin-coated on an ITO substrate in dichloromethane containing 0.1 M TBAP at a scan rate of 100 mV s^{-1} .

filled up, consequently forming another charge-transporting channel, resulting in the observed high-conductivity state (Fig. 6a and c). The result is also verified by experimental data. The conformational effect is supported by the UV-vis spectra measurements of the P4VPCz5 thin film in the before-conductivity (OFF state) and after-conductivity (ON1 state) states. As shown in Fig. 6b, after a voltage sweep of 0 to -3.0 V with a liquid Hg droplet instead of the Al electrode, a slight but evident red shift could be seen, arising from the ordered π - π stacking of the carbazole groups.^{7,14,15} Besides, the second switching may be explained by the formation of a trapping level in the device.^{5,6} It can be rationalized by evaluating the HOMO and LUMO energy levels of the P4VPCz combined with the work function of the ITO and Al electrode, as shown in Fig. 7. It can be confirmed that the charge transfer (CT) between the carbazole and pyridine moieties is relatively weak because no obvious change was observed with different D/A ratios from the UV-vis and CV results. For a *p*-type semiconductor material, it is easier for the fabricated device to achieve current flow when the ITO is enriched with enough holes. Herein, the electron-withdrawing pyridines are likely to serve as the hole-blocking moieties in the active layer and would be filled with holes to full, under an electric field.¹⁶ The V_{th} s of P4VPCz5 (around -3.5 V) and P4VPCz2 (around -3.3 V) indicated their fabricated devices have almost the same switching voltage, which is due to the same energy gaps lying in the ITO and their own HOMO orbits.

Table 1 Thermal, optical and electrochemical properties of the **P4VPCz**

	TGA (°C)	λ_{Edge} (nm)	E_g (eV)	E_{ox} (eV)	HOMO (eV)	LUMO (eV)
P4VPCz2	270	395.1	3.14	1.38	-5.56	-2.42
P4VPCz5	272	395.5	3.14	1.36	-5.58	-2.44
P4VPCz8	275	395.3	3.14	1.28	-5.66	-2.52

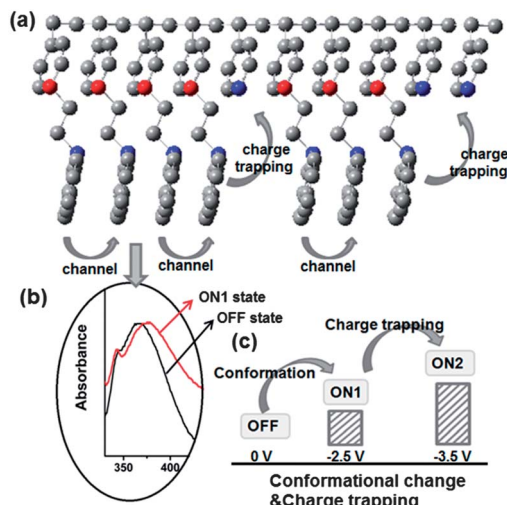


Fig. 6 (a and c) Schematic diagram of the charge carrier transport process in the **P4VPCz5**-based memory device. (b) UV-visible spectra of the **P4VPCz5** thin films in the OFF and ON1 state on an ITO substrate; the ON1 state was programmed by using a removable liquid Hg droplet as the top electrode.

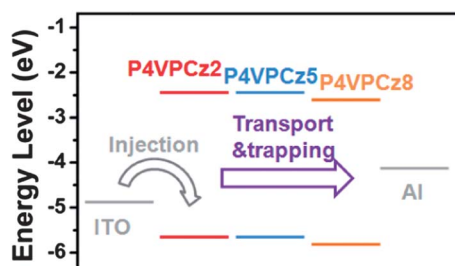


Fig. 7 Molecular simulation of the HOMO and LUMO energy levels for **P4VPCz** along with the work function of the electrodes.

Therefore, the double switching process in **P4VPCz5** is well explained.

The doped ions could help to balance charge injection and transport within the active layer to improve the device stability performance, so the devices based on **P4VPCz2** (or **P4VPCz5**) show a very uniform and stable V_{th} s (Fig. S7 and S8, ESI[†]). Besides, the OFF state current of **P4VPCz5** is increased with the increasing of the doped ions. Yet, in further increasing the content of the carbazole moieties and doped ions, the **P4VPCz8** thin film based devices show only a single high-conductivity state, with no switching phenomenon. The characteristics of the high conductance state of the **P4VPCz8** device completely showed an ohmic trend (Fig. 8).¹⁷ The **P4VPCz8** has a high

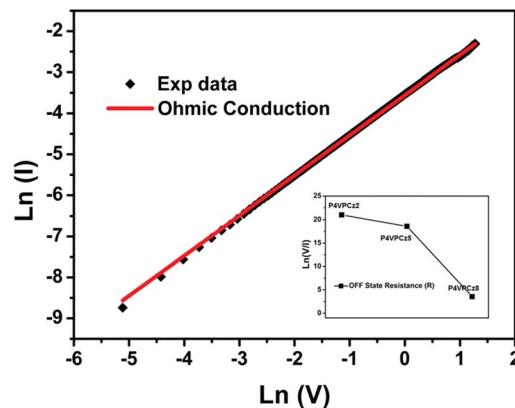


Fig. 8 Analysis of the fitted I - V characteristics of the ITO/**P4VPCz8**/Al device in the ON state, the inset is the **P4VPCz** resistance (R) analysis in the OFF state.

concentration of carbazole moieties, as well as the doped ions, which made it easier to form pathways for charge hopping between neighboring carbazole units, leading to initially exhibit the ON state. The I - V curves of the **P4VPCz2** and **P4VPCz5** devices were also analyzed with appropriate theoretical conduction models to clarify the carrier transport and mechanism using thermionic emission limited and ohmic current model (Fig. S9 and S10, ESI[†]). The OFF state (or ON1 state) current, below the threshold voltage might be attributed to the thermally generated charge carriers through the straight line fitting on the plot of $\ln(I)$ versus $V^{1/2}$, while the ON state (or ON2 state) current shows a linear fitting plot of $\ln(I)$ versus $\ln(V)$, based on the ohmic current model. From the systematic electrical characterization and analysis, it is better to understand the different switching behavior of the **P4VPCz** devices based on copolymers with different compositions.

Conclusions

We have demonstrated ternary memory properties controlled by a dual mechanism, achieved with **P4VPCz** copolymers. Through tuning the content of flexible lateral carbazole moieties and the doped ions, the devices based on **P4VPCz** were able to show various electrical behaviors such as bistable switching, tristable switching and a conductor behavior. The **P4VPCz2** only exhibited bistable states with a nonvolatile WORM characteristic due to charge trapping under the electrical field. However, the **P4VPCz5** showed a double switching behavior (tristable states) that could mainly be attributed to the conformational change and charge trapping, successively. It is believed that

our study may offer a guideline for the design of practical polymer-based multilevel devices *via* introducing more than one mechanism in the active materials and the double switching process in the ternary device provides clarification of this proposal.

Experimental section

Materials

Carbazole (99%), 2-chloroethanol (99%), phosphorus tribromide (PBr₃) (99%), poly(4-vinylpyridine) (Mw *ca.* 60 000), potassium hydroxide (KOH) (99%), and the solvents were all purchased from the Shanghai Chemical Reagent Co. Ltd. *N,N*-dimethylformamide (DMF) was purified by reduced pressure distillation. The other reagents were used as received without any further purification.

Synthesis of 2-(9*H*-carbazol-9-yl)ethanol

A mixture of carbazole (6.68 g, 40 mmol), 2-chloroethanol (7.2 mL, 52 mmol), KOH (14.0 g, 0.25 mol), and DMF (80 mL) was stirred at 50 °C for 12 hours. After the reaction was completed, the mixture was poured into a large excess of water, and suspended for 6 hours. The precipitated product was filtered and further purified *via* a silica gel column with chloroform and petroleum ether (volume ratio = 2 : 1), yield 80%. ¹H NMR (DMSO-*d*₆, 400 MHz), δ (ppm): 3.74–3.85 (m, 2H), 4.45 (dd, *J* = 4.41, 7.07 Hz, 2H), 5.51 (t, *J* = 5.37 Hz, 1H), 7.15–7.26 (m, 2H), 7.40–7.50 (m, 2H), 7.65 (dd, *J* = 4.70, 10.23 Hz, 2H), 8.10–8.21 (m, 2H).

Synthesis of 9-(2-bromoethyl)-9*H*-carbazole (BCz)

The DMF (purified) solution containing 2-(9*H*-carbazol-9-yl) ethanol (2.07 g, 20 mmol) in a 50 mL flask was purged with argon, and then stirred at 0 °C. Then PBr₃ (2.8 mL)–DMF (5 mL) was slowly added. The mixture was stirred at room temperature for about 12 hours. After the reaction, a saturated Na₂CO₃ solution was slowly added to remove excess PBr₃. The mixture was extracted with CH₂Cl₂, dried over Na₂SO₄ and then the solvent was evaporated. The final product was obtained through a silica gel column (ethyl acetate: petroleum ether = 1 : 2) to give a colorless liquid. Yield: 85%. ¹H NMR (DMSO-*d*₆, 400 MHz), δ (ppm): 3.92 (t, *J* = 6.31 Hz, 2H), 4.85 (t, *J* = 6.31 Hz, 2H), 7.22 (t, *J* = 7.46 Hz, 2H), 7.46 (t, *J* = 7.68 Hz, 2H), 7.66 (d, *J* = 8.20 Hz, 2H), 8.16 (d, *J* = 7.73 Hz, 2H).

Synthesis of P4VPCz

A mixture of poly(4-vinylpyridine) (200 mg, 3.3 mmol) (Mw *ca.* 60 000) and 9-(2-bromobutyl)-9*H*-carbazole (540–1620 mg, 2.0–6.0 mmol) in 4.0 mL of DMF–CH₃OH (1 : 1) was stirred at 50 °C in a round-bottom flask for one week. The mixture became clear after 3 h and then turned red 3 days later. Toluene was used to precipitate the brownish solid product, followed by a Soxhlet extraction for 3 days, giving the product after vacuum drying. ¹H NMR (DMSO-*d*₆, 400 MHz) δ (ppm): 1.04–1.92, 4.65–5.28, 6.32–6.92, 6.98–7.55, 7.90–8.62. This polymer was soluble in DMSO and DMF.

Instruments

The ¹H NMR spectra were obtained on an Inova 400 MHz FT-NMR spectrometer. The UV-vis absorption spectra were recorded on a Perkin Elmer Lambda-17 spectrophotometer at room temperature. Thermogravimetric analysis (TGA) was conducted on a TA instrument Dynamic TGA 2950 at a heating rate of 20 °C min⁻¹ under a nitrogen flow rate of 100 mL min⁻¹. Cyclic voltammetry was performed at room temperature using an ITO working electrode, a reference electrode of Ag/AgCl, and a counter electrode (Pt wire) at a scanning rate of 100 mV s⁻¹ (CorrTest CS Electrochemical Workstation analyzer) in a solution of tetrabutylammonium perchlorate (TBAP) in dichloromethane (0.1 M). The SEM images were taken on a Hitachi S-4700 scanning electron microscope. The atomic force microscopy (AFM) measurements were performed by using a MFP-3DTM (Digital Instruments/Asylum Research) AFM instrument in the tapping mode.

Device fabrication

The indium tin oxide (ITO) glass was pre-cleaned sequentially with deionized water, acetone and ethanol in an ultrasonic bath, each for 20 min. The polymer was dissolved in *N,N*-dimethylformamide (15 mg mL⁻¹) and filtered through micro-filters with a pinhole size of 0.22 mm. Thereafter, the solutions were spin-coated onto ITO at 2000 rpm and the solvent was removed in a vacuum chamber at 10⁻¹ Pa and 50 °C for 12 h. The thickness of the polymer layer was about 80 nm. Finally, the top Al electrode, 100 nm thick was thermally evaporated through a shadow mask under a pressure of 5 × 10⁻⁶ Torr. The active area of each cell was 0.126 mm² (a nummular point with a radius of 0.2 mm). All the electrical measurements of the devices were characterized under a nitrogen atmosphere, using an HP 4145B semiconductor parameter analyzer.

Acknowledgements

This work was financially supported by the NSF of China (21076134, 21176164, 21206102 and 21336005), the NSF of Jiangsu Province (BK2010208 and BE2013052), a project of the Department of Education of Jiangsu Province (12KJB430011), Suzhou Nano-project (ZXG2012023) and Project supported by the Specialized Research Fund for the Doctoral Program of Higher Education of China (Grant no. 20113201130003 and 20123201120005). This is also a project funded by the Priority Academic Program Development of the Jiangsu Higher Education Institutions (PAPD).

Notes and references

- (a) Y. Yang, J. Ouyang, L. Ma, R. J. H. Tseng and C. W. Chu, *Adv. Funct. Mater.*, 2006, **16**, 1001; (b) C. L. Liu and W. C. Chen, *Polym. Chem.*, 2011, **2**, 2169; (c) Q. D. Ling, D. J. Liaw, C. Zhu, D. S. H. Chan, E. T. Kang and K. G. Neoh, *Prog. Polym. Sci.*, 2008, **33**, 917; (d) A. Bandyopadhyay, S. Sahu and M. Higuchi, *J. Am. Chem. Soc.*, 2011, **133**, 1168; (e) D. M. Kim, S. park, T. J. Lee,

- S. G. Hahm, K. Kim, J. C. Kim, W. Kwon and M. Ree, *Langmuir*, 2009, **25**, 11713; (f) J. Lin and D. Ma, *J. Appl. Phys.*, 2008, **103**, 024507; (g) N. Y. Fan, H. F. Liu, Q. H. Zhou, H. Zhuang, Y. Li, H. Li, Q. F. Xu, N. J. Li and J. M. Lu, *J. Mater. Chem.*, 2012, **22**, 19957.
- 2 (a) M. Hasan, R. Dong, H. J. Choi, D. S. Lee, D. J. Seong, M. B. Pyun and H. Hwang, *Appl. Phys. Lett.*, 2008, **92**, 202102; (b) S. Kim, K. P. Biju, M. Jo, S. Jung, J. Park, J. Lee, W. Lee, J. Shin, S. Park and H. Hwang, *IEEE Electron Device Lett.*, 2011, **32**, 671.
- 3 (a) H. Li, Q. F. Xu, N. J. Li, R. Sun, J. F. Ge, J. M. Lu, H. W. Gu and F. Yan, *J. Am. Chem. Soc.*, 2010, **132**, 5542; (b) S. F. Miao, H. Li, Q. F. Xu, Y. Y. Li, S. J. Ji, N. J. Li, L. H. Wang, J. W. Zheng and J. M. Lu, *Adv. Mater.*, 2012, **24**, 6210; (c) H. Zhuang, Q. J. Zhang, Y. X. Zhu, X. F. Xu, H. F. Liu, N. J. Li, Q. F. Xu, H. Li, J. M. Lu and L. H. Wang, *J. Mater. Chem. C*, 2013, **1**, 3816; (d) S. F. Miao, Y. X. Zhu, H. Zhuang, X. P. Xu, H. Li, R. Su, N. J. Li, S. J. Ji and J. M. Lu, *J. Mater. Chem. C*, 2013, **1**, 2320.
- 4 (a) S. J. Liu, P. Wang, Q. Zhao, H. Y. Yang, J. Wong, H. B. Sun, X. C. Dong, W. P. Lin and W. Huang, *Adv. Mater.*, 2012, **24**, 2901; (b) G. Liu, D. J. Liaw, W. Y. Lee, Q. D. Ling, C. X. Zhu, D. S. H. Chan, E. T. Kang and K. G. Neoh, *Philos. Trans. R. Soc. London, Ser. A*, 2009, **367**, 4203; (c) H. Zhuang, X. P. Xu, Y. H. Liu, Q. H. Zhou, X. F. Xu, H. Li, Q. F. Xu, N. J. Li, J. M. Lu and L. H. Wang, *J. Phys. Chem. C*, 2012, **116**, 25546.
- 5 (a) Q. D. Ling, Y. Song, S. L. Lim, E. Y. H. Teo, Y. P. Tan, C. X. Zhu, D. S. H. Chan, D. L. Kwong, E. T. Kang and K. G. Neoh, *Angew. Chem., Int. Ed.*, 2006, **45**, 2947; (b) G. Liu, Q. D. Ling, E. T. Kang, K. G. Neoh and D. J. Liaw, *J. Appl. Phys.*, 2007, **102**, 024502.
- 6 (a) X. D. Zhuang, Y. Chen, B. X. Li, D. G. Ma, B. Zhang and Y. Li, *Chem. Mater.*, 2010, **22**, 4455; (b) H. Li, N. J. Li, H. W. Gu, Q. F. Xu, F. Yan, J. M. Lu, X. W. Xia, J. F. Ge and L. H. Wang, *J. Phys. Chem. C*, 2010, **114**, 6117; (c) G. Liu, Q. D. Ling, E. Y. H. Teo, C. X. Zhu, D. S. H. Chan, K. G. Neoh and E. T. Kang, *ACS Nano*, 2009, **3**, 1929.
- 7 (a) S. L. Lim, Q. Ling, E. Y. H. Teo, C. X. Zhu, D. S. H. Chan, E. T. Kang and K. G. Neoh, *Chem. Mater.*, 2007, **19**, 5148; (b) W. S. Kwon, B. C. Ahn, D. M. Kim, Y. G. Ko, S. G. Hahm, Y. K. Kim, H. J. Kim and M. Ree, *J. Phys. Chem. C*, 2011, **115**, 19355; (c) Y. H. Liu, N. J. Li, X. W. Xia, Q. F. Xu, J. F. Ge and J. M. Lu, *Mater. Chem. Phys.*, 2010, **123**, 685.
- 8 (a) T. W. Kim, S. H. Oh, J. Lee, H. Choi, G. Wang, J. Park, D. Y. Kim, H. Hwang and T. Lee, *Org. Electron.*, 2010, **11**, 109; (b) Y. G. Ko, W. Kwon, D. M. Kim, K. Kim, Y. S. Gal and M. Ree, *Polym. Chem.*, 2012, **3**, 2028.
- 9 (a) B. L. Hu, X. J. Zhu, X. X. Chen, L. Pan, S. S. Peng, Y. Z. Wu, J. Shang, G. Liu, Q. Yan and R. W. Li, *J. Am. Chem. Soc.*, 2012, **134**, 17408; (b) A. Pereira, H. M. C. Barbosa, H. M. G. Correia, L. Marques and M. M. D. Ramos, *J. Mater. Chem.*, 2010, **20**, 9470.
- 10 (a) Y. K. Fang, C. L. Liu, C. Li, C. J. Lin, R. Mezzenga and W. C. Chen, *Adv. Funct. Mater.*, 2010, **20**, 3012; (b) X.-D. Zhuang, Y. Chen, G. Liu, B. Zhang, K. G. Neoh, E. T. Kang, C. X. Zhu, Y. X. Li and L. J. Niu, *Adv. Funct. Mater.*, 2010, **20**, 2916.
- 11 (a) Y. K. Fang, C. L. Liu and W. C. Chen, *J. Mater. Chem.*, 2011, **21**, 4778; (b) S. L. Lian, C. L. Lin and W. C. Chen, *ACS Appl. Mater. Interfaces*, 2011, **3**, 4504.
- 12 (a) X. D. Zhuang, Y. Chen, B. X. Li, D. G. Ma, B. Zhang and Y. Li, *Chem. Mater.*, 2010, **22**, 4455; (b) Y. K. Fang, C. L. Liu, C. Li, C. J. Lin, R. Mezzenga and W. C. Chen, *Adv. Funct. Mater.*, 2010, **20**, 3012.
- 13 Q. D. Ling, D. J. Liaw, E. Y. H. Teo, C. X. Zhu, D. S. H. Chan, E. T. Kang and K. G. Neoh, *Polymer*, 2007, **48**, 5182.
- 14 (a) G. Safoula, K. Napo, J. C. Bernede, S. Touihri and K. Alimi, *Eur. Polym. J.*, 2001, **37**, 843; (b) L. H. Xie, Q. D. Ling, X. Y. Hou and W. Huang, *J. Am. Chem. Soc.*, 2008, **130**, 2120.
- 15 B. Zhuang, Y. J. Chen, Y. F. Zhang, X. D. Chen, Z. G. Chi, J. Yang, J. M. Ou, M. Q. Zhang, D. H. Li, D. Wang, M. K. Liu and J. Y. Zhou, *Phys. Chem. Chem. Phys.*, 2012, **14**, 4640.
- 16 S. L. Lian, C. L. Liu and W. C. Chen, *ACS Appl. Mater. Interfaces*, 2011, **3**, 4504.
- 17 (a) T. J. Lee, S. Park, S. G. Hahm, D. M. Kim, K. Kim, J. Kim, W. Kwon, Y. Kim, T. Chang and M. Ree, *J. Phys. Chem. C*, 2009, **113**, 3855; (b) J. Lin and D. G. Ma, *Appl. Phys. Lett.*, 2008, **93**, 093505.